Inorganic Chemistry

Article

pubs.acs.org/IC

Low-Concentration Eu^{2+}-Doped $SrAlSi_4N_7$: Ce^{3+} Yellow Phosphor for wLEDs with Improved Color-Rendering Index

Liangliang Zhang,[†] Jiahua Zhang,*[,†] Guo-Hui Pan,[†] Xia Zhang,[†] Zhendong Hao,[†] Yongshi Luo,[†] and Huajun Wu[†]

[†]State Key Laboratory of Luminescence and Applications, Changchun Institute of Optics, Fine Mechanics and Physics, Chinese Academy of Sciences, 3888 Eastern South Lake Road, Changchun 130033, China

Supporting Information

ABSTRACT: Luminescence property of low-concentration Eu^{2+}-doped $SrAlSi_4N_7$:Ce^{3+} yellow phosphor is reported in this paper. Three optical centers Ce1, Ce2, and Eu2 are observed in the phosphor. Deconvolution of emission spectrum confirms the three centers to be green (530 nm), yellow (580 nm), and red (630 nm), respectively. This property promises considerable improvement of color-rendering property of a white light-emitting diode (wLED). For example, color-rendering index (CRI) of wLED fabricated by combining a blue LED chip and $SrAlSi_4N_7$:$0.05Ce^{3+}$,$0.01Eu^{2+}$ phosphor reaches 88. A competitive energy transfer process between Ce1−Ce2 and Ce1−Eu2 is confirmed based on Inokuti−Hirayama formula. Ratio of energy transfer rate between Ce1−Ce2 and Ce1−Eu2 ($W_{Ce1-Eu2}/W_{Ce1-Ce2}$) is calculated to be 2.0. This result reveals the effect of Eu^{2+} concentration on quantity of green and red components in $SrAlSi_4N_7$:Ce^{3+},Eu^{2+} phosphor.

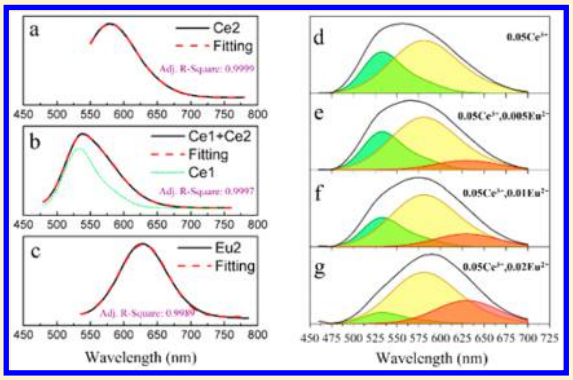

INTRODUCTION

Blue light-emitting diode won its Nobel Prize in physics in 2014 for a world-changing advancement in white light-emitting diode (wLED), and this industry developed into a $20 billion lighting market nowadays. However, choke point is encountered by wLED for its poor color-rendering property.[1,2] For example, wLED by using a blue InGaN chip to pump YAG:Ce^{3+} yellow phosphor only shows color-rendering index (CRI) less than 80.[3] Such a CRI is too low to be applied for daily illumination. Thus, great efforts have been paid to explore new phosphors for high CRI in recent years.[4−6] $SrAlSi_4N_7$:Ce^{3+} is one of the interesting yellow phosphors with luminescence property similar to YAG:Ce^{3+}. The emission bandwidth of $SrAlSi_4N_7$:Ce^{3+} is 115 nm[7] and is much broader than that of YAG:Ce^{3+}. This broad band emission property of $SrAlSi_4N_7$:Ce^{3+} promises a wLED with CRI of 81. Thus, $SrAlSi_4N_7$:Ce^{3+} is believed to be a possible substitute for YAG:Ce^{3+} phosphor. However, further improvement of $SrAlSi_4N_7$:Ce^{3+} for higher CRI is still expected. The key issue is to increase red component in the emission spectrum.

There are two technological solutions to increase red component of a phosphor. One method is shifting the emission to longer wavelength by introducing larger ions. For example, Gd^{3+} [8] is introduced to substitute for Y^{3+}, and (Ga^{3+}, In^{3+})[9] is introduced to substitute for Al^{3+} in YAG:Ce^{3+}. The emission of YAG:Ce^{3+} shifts from 535 to 575 nm,[10] and CRI increases to 80. However, increase of CRI is limited by this method for the decrease of green component. Worse still, the introduced foreign ions quench the emission intensity severely. Another way to enhance red emission is by introducing new red optical centers. For example, Ce^{3+} codoped with Pr^{3+}, Eu^{3+}, or Mn^{2+} in YAG.[11−14] CRI of Pr^{3+} codoped YAG:Ce^{3+} increases to 83[15] with a new red emission band at 610 nm. These red centers are always transition forbidden and show weak absorption themselves. Intensity of red centers depends on the energy transfer processes. Thus, an effective energy transfer results in obvious increased red component.

On the basis of the above-mentioned methods, efforts have been paid to increase red component in $SrAlSi_4N_7$:Ce^{3+}. W. Park et al. replace Sr^{2+} by Ba^{2+} and Ca^{2+} and replace Al^{3+} by Y^{3+}, La^{3+}, and Lu^{3+} in $SrAlSi_4N_7$.[16] Unfortunately, the substitution changes the space group into $p6_3mc$ and results in a blue-shift of emission. J. Run et al.[17] introduce Li^+ to offer charge compensation for Ce^{3+} in $SrAlSi_4N_7$. The emission of Ce^{3+}/Li^+ doped $SrAlSi_4N_7$ shifts to 565 nm. Compared with 555 nm emission of Ce^{3+}-doped $SrAlSi_4N_7$, such a 10 nm shift makes little sense to the improvement of CRI. The red shift of Ce^{3+} emission is ascribed to the increase of Ce^{3+} concentration (quenching concentration increases from 3% to 5%). Z. Zhang et al.[18,19] introduce new optical centers like Yb^{2+}, Sm^{2+}, Tb^{3+}, and Pr^{3+} into $SrAlSi_4N_7$. Yb^{2+} shows emission at 600 nm, Sm^{2+} shows emission at 610 and 650 nm, and Pr^{3+} shows emission at 612 nm. Unfortunately, all these works show limited improvement of CRI.

Received: June 24, 2016
Published: September 12, 2016

DOI: 10.1021/acs.inorgchem.6b01490
Inorg. Chem. 2016, 55, 9736−9741

In this paper, we codoped Eu^{2+} into $SrAlSi_4N_7:Ce^{3+}$ to increase the red component. Eu^{2+} has been reported to be a red center in $SrAlSi_4N_7$.[20−22] Eu^{2+} ion is transition-allowed and shows intense absorption and emission by itself. This means that emission intensity of Eu^{2+} does not depend on the Ce^{3+}−Eu^{2+} energy transfer process. This character promises $SrAlSi_4N_7:Ce^{3+},Eu^{2+}$ phosphor many amazing proprieties like increased absorption and bandwidth. Three optical centers are observed in $SrAlSi_4N_7:Ce^{3+},Eu^{2+}$ phosphors and are confirmed to be green, yellow, and red, respectively. Such three optical centers endow a great improvement of CRI. Energy transfer processes between different optical centers are also discussed in detail to understand the effect of Eu^{2+} concentration on optical property.

EXPERIMENTAL DETAILS

Synthesis. Undoped and Ce^{3+}, Eu^{2+} codoped $SrAlSi_4N_7$ were synthesized by employing carbothermal reduction and nitridation method. $SrCO_3$ (99.99%), α-Si_3N_4 (98%), AlN (99.9%), and CeO_2 (99.99%) were weighted as starting materials. Fine graphite powder (99.9%) was used as carbon source with amount of 200 mol % of Sr atoms. The raw materials were ground in an agate mortar and pressed into a graphite crucible. Then the crucible was positioned in a tube furnace and sintered at 1600 °C for 10 h under a N_2 flow.

Characterization. X-ray diffraction (XRD) patterns were collected in a powder diffractometer (Bruker, D8 Focus, Cu Kα, 40 kV, 40 mA). The XRD data were collected in range of 20−50° with count time of 3 s/step. The instrumental broadening was measured by using standard Si. The morphology was investigated by using a field emission scanning electron microscopy (Hitachi, S-4800, 25KV). The excitation and emission spectra were measured using HITACHI F-4500 spectrometer with a 200 W Xe Lamp. The excitation and emission slits were both set at 2.5 nm. Response function was determined by using Rhodamine B solution and a calibration halogen lamp. The optical properties of wLED were measured by a microfiber spectrometer (Ocean Optics, USB4000). The decay curves were measured by FL920 fluorimeter (Edinburgh Instruments) with a hydrogen lamp (nF900). Pulse time of the light source is 1 ns.

RESULTS AND DISCUSSION

Structure. XRD pattern of $SrAlSi_4N_7:0.05Ce^{3+},0.01Eu^{2+}$ is shown in Figure 1. The intensity distribution of XRD pattern (Figure 1c) is quite different from the standard one (Figure 1a) with (4 2 0) peak extremely high. This is ascribed to the preferred growth perpendicular to (4 2 0) lattice plane.[7] As a result, the particles grow into a rod shape, as shown in Figure 1. This phenomenon is also reported by other researchers, and we revealed the reason for this phenomenon in our previous work. It must be pointed out that the preferred growth will not change the position of XRD peaks. So we still confirm a pure $SrAlSi_4N_7$ phase by comparing the position of XRD pattern with the standard one. To eliminate the negative effect caused by preferred orientation, the sample is granulated before XRD measurement. The granulation progress is expected to make the particles distribute randomly. As shown in Figure 1b, XRD pattern measured by the granulated sample shows suppressed (4 2 0) peak compared with the ungranulated one. Influence of preferred orientation to luminesce property is not appreciable.

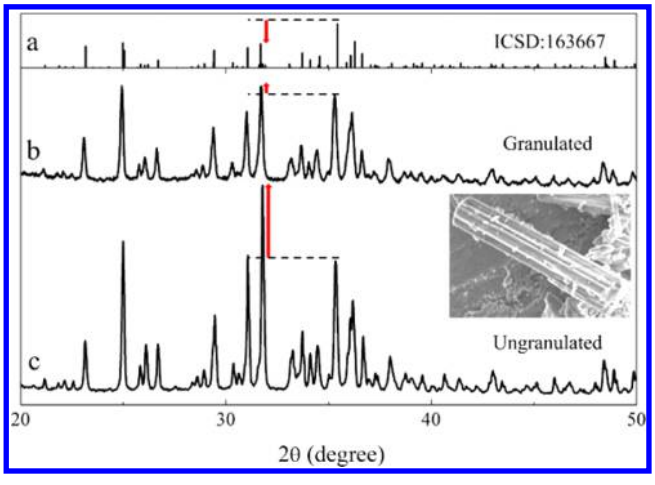

Figure 1. (a) Standard XRD pattern of $SrAlSi_4N_7$. (b, c) XRD pattern of granulated and ungranulated $SrAlSi_4N_7:0.05Ce^{3+},0.01Eu^{2+}$ powder.

Color-Tunable Property and Application in wLED. Emission spectra of $SrAlSi_4N_7:0.05Ce^{3+},yEu^{2+}$ samples are shown in Figure 2a. With increasing concentration of Eu^{2+}, emission of $SrAlSi_4N_7:0.05Ce^{3+},yEu^{2+}$ shifts from 550 to 610 nm. Such a 60 nm shift allows highly color-tunable phosphor. However, heavy Eu^{2+}-doped phosphors are so red that it failed to realize a white light output. Since this paper is focused on improvement of CRI of wLED, we will mainly study on dilute Eu^{2+}-doped samples, which is a yellow phosphor. The full width at half-maximum (FWHM) and wavelength of emission of dilute Eu^{2+}-doped $SrAlSi_4N_7:0.05Ce^{3+}$ phosphors are shown in Figure 2d. It can be found that $SrAlSi_4N_7:0.05Ce^{3+},0.01Eu^{2+}$ shows the widest emission band with FWHM of 119 nm. The efficiency of wLED fabricated by $SrAlSi_4N_7:0.05Ce^{3+},0.01Eu^{2+}$ is 11 lm/W, and efficiency of wLED fabricated by $SrAlSi_4N_7:0.05Ce^{3+}$ is also 11 lm/W. This indicates that efficiencies do not change seriously by low-concentration doped Eu^{2+}. The low efficiency of wLED is caused by the residual carbon in the phosphor. It is a common phenomenon in carbothermal reduction method when preparing the samples.[7]

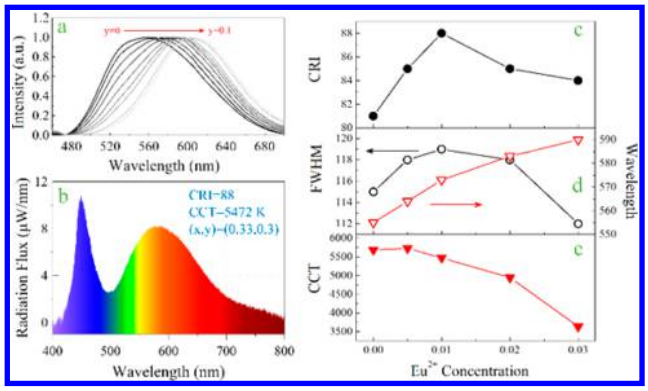

Figure 2. (a, d) Emission spectra, FWHM, and emission wavelength of $SrAlSi_4N_7:0.05Ce^{3+},yEu^{2+}$ samples excited by 450 nm. (b) Radiant flux spectra of wLED by combining blue LED chip and $SrAlSi_4N_7:0.05Ce^{3+},0.01Eu^{2+}$ phosphor. (c, e) CRI and color temperature of wLEDs by using $SrAlSi_4N_7:0.05Ce^{3+},yEu^{2+}$ phosphors.

Figure 2c,e shows optical properties of wLEDs by using $SrAlSi_4N_7:0.05Ce^{3+},yEu^{2+}$ phosphors. wLED by using $SrAlSi_4N_7:0.05Ce^{3+},0.005Eu^{2+}$ shows higher CRI compared with $SrAlSi_4N_7:0.05Ce^{3+}$. $SrAlSi_4N_7:0.05Ce^{3+},0.01Eu^{2+}$ shows further improvement of CRI to 88. Radiant flux spectra of wLED by using $SrAlSi_4N_7:0.05Ce^{3+},0.01Eu^{2+}$ phosphor is shown in Figure 2b. When $y > 0.01$, CRI decline slightly, but the light is warmer with correlated color temperature (CCT) decrease from 5472 to 3632 K. Thus, low-concentration doped Eu^{2+} is

DOI: 10.1021/acs.inorgchem.6b01490
Inorg. Chem. 2016, 55, 9736−9741

favorable to application in wLEDs requiring high CRI, while heavier-doped sample is favorable to wLEDs in need of low CCT (Figure 2d,e).

Strong association is found between CRI and emission FWHM. As shown in Figure 2c,d, $SrAlSi_4N_7$:0.05Ce^{3+},0.01Eu^{2+} shows best CRI and largest FWHM. This indicates that CRI of wLEDs are depend on the FWHM of phosphor. This is because both the green and red component contribute to CRI. When $0 < y \leq 0.01$, FWHM increases as result of increased red component. When $y > 0.01$, green component decreases rapidly, and FWHM decreased. Thus, increased Eu^{2+} concentration results in decrease of green component and increase of red component. This is the critical progress that influence CRI of wLEDs. So we will focus on the mechanism of how Eu^{2+} ion affects the relative quantity of green and red components.

First, we need to deconvolute the emission spectrum to determine luminescence centers in $SrAlSi_4N_7$:Ce^{3+},Eu^{2+}. As reported in our previous works,[7] emission of $SrAlSi_4N_7$:0.05Ce^{3+} is composed of two sub-bands, which originated from Ce1 and Ce2 optical centers, respectively. We can excite Ce2 center alone by a 520 nm green light, as shown in Figure 3a. Only half of Ce2 spectrum is measured, since the emission

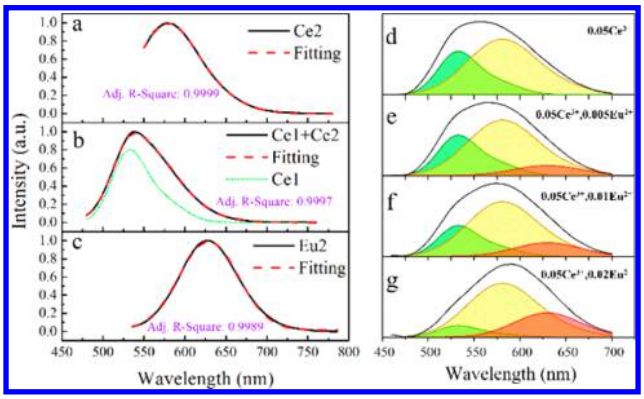

Figure 3. Gaussian fitting of emission peaks of $SrAlSi_4N_7$:0.05Ce^{3+} excited by 520 nm (a) and 450 nm (b). Gaussian fitting of emission peaks of $SrAlSi_4N_7$:0.05Eu^{2+} excited by 450 nm (c). Emission spectra of $SrAlSi_4N_7$:0.05Ce^{3+},yEu^{2+} samples excited by 450 nm with deconvolved sub-bands of Ce1, Ce2, and Eu2 centers (d–g).

spectrum is overlapped with excitation light. However, the whole spectrum can also be got by fitting the measured spectrum with two Gaussian functions (Ce^{3+} emission is characteristic of two Gaussian peaks). The normalized peak function of Ce2 is

$$\mathrm{Ce2}(x) = \frac{91.976}{74.446} e^{-2\left(\frac{x-580}{74.446}\right)^2} + \frac{7.87}{63.243} e^{-2\left(\frac{x-650}{63.243}\right)^2} \quad (1)$$

When excited by 450 nm, emission of $SrAlSi_4N_7$:0.05Ce^{3+} consists of emission from both Ce1 and Ce2, as shown in Figure 3b. Fitting of the spectrum with two Gaussian functions and Ce2 function, we get the expression of Ce1 emission. The normalized peak function of Ce1 is

$$\mathrm{Ce1}(x) = \frac{45.264}{40.608} e^{-2\left(\frac{x-530}{40.608}\right)^2} + \frac{21.318}{52.721} e^{-2\left(\frac{x-570}{52.721}\right)^2} \quad (2)$$

When Eu^{2+} is codoped, a new red sub-band occurs. This sub-band is ascribed to Eu2 emission, since Eu1 luminescence is reported to be ~500 nm and can hardly be recognized at room temperature.[20,21] Expression of Eu2 emission can be got by fitting emission of $SrAlSi_4N_7$:0.01Eu^{2+} with a single Gaussian function (Eu^{2+} emission is characteristic of one Gaussian peak), as shown in Figure 3c. The normalized peak function of Eu2 is

$$\mathrm{Eu2}(x) = \frac{88.649}{72.217} e^{-2\left(\frac{x-630}{72.217}\right)^2} \quad (3)$$

These functions show that Ce1 is a green luminescence center with a 530 nm emission, Ce2 is a yellow center with a 580 nm emission, and Eu2 is a red center with a 630 nm emission. Such three components are critical for good color-rendering property of a wLED. Three functions of Ce1, Ce2, and Eu2 are introduced to fit the emission of $SrAlSi_4N_7$:0.05Ce^{3+},yEu^{2+}, as shown in Figure 3d–g. This method visualizes the relative quantity of green, yellow, and red components in different samples. Obviously, the green component decreases rapidly, while red component increases. As a matter of fact, decrease of green component is not desirable for a further decrease of CRI. So we are interested in the progress that results in a diminished Ce1 emission (green component).

Energy Transfer. Figure 4a is excitation spectrum of $SrAlSi_4N_7$:0.05Ce^{3+} monitoring at 630 nm. 630 nm emission is

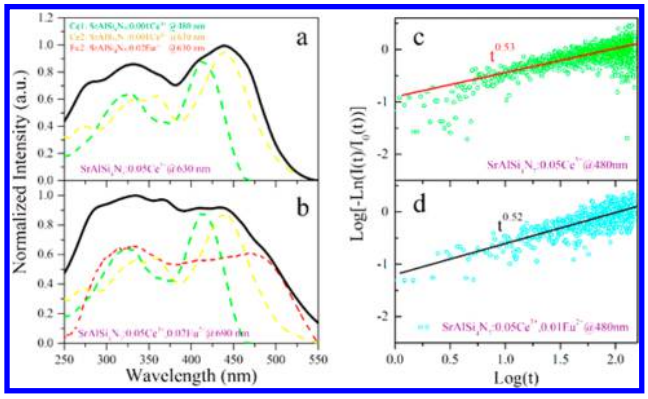

Figure 4. Excitation spectra of $SrAlSi_4N_7$:0.05Ce^{3+} monitoring at 630 nm (a) and $SrAlSi_4N_7$:0.05Ce^{3+},0.02Eu^{2+} monitoring at 690 nm (b). Excitation spectra of Ce1 and Ce2 are measured by monitoring 480 and 630 nm emission of $SrAlSi_4N_7$:0.001Ce^{3+}. Excitation spectra of Eu2 are measured by monitoring 630 nm emission of $SrAlSi_4N_7$:0.02Eu^{2+}. Relationship between $\log[-\ln(I(t)/I_0(t))]$ and $\log(t)$ of $SrAlSi_4N_7$:0.05Ce^{3+} (c) and $SrAlSi_4N_7$:0.05Ce^{3+},0.01Eu^{2+} (d).

mainly from Ce2 center; Ce1 emission is undetectable at this point. So the excitation spectrum is expected to coincide with the excitation bands of Ce2. However, the excitation spectrum consists of characteristic excitation bands of both Ce1 and Ce2, as shown in Figure 4a. This indicates energy transfer from Ce1 to Ce2. Figure 4b is excitation spectrum of SrAlSi4N7:0.05-Ce3^{+},0.02Eu^{2+} monitoring 690 nm. This wavelength is mainly from Eu2 emission. However, excitation bands of Ce1 and Ce2 are also detected, as shown in Figure 4b. This indicates energy transfer from both Ce1 and Ce2 to Eu2. Thus, we can conclude that diminished Ce1 emission is originated from energy transfer process from Ce1 to Ce2 and Eu2. With increasing Eu^{2+} concentration, the energy transfer rate from Ce1 to Eu2 increases, and emission of Ce1 decreases monotonically. When concentration of Eu^{2+} exceeds 0.03, emission of Ce1 (green component) is almost unobservable. Since Eu2 can also be effectively excited by 450 nm, emitted photon from Eu^{2+} ion is

DOI: 10.1021/acs.inorgchem.6b01490
Inorg. Chem. 2016, 55, 9736–9741

originated from both energy transfer process and absorption by itself. Thus, the increased intensity of Eu2 (red component) is ascribed from both increased absorption of Eu^{2+} and the transferred energy.

It has been proved that there is energy transfer between Ce1−Ce2 and Ce1−Eu2. The electric interaction type of Ce1−Ce2 and Ce1−Eu2 can be proved to be both dipole−dipole. According to Inokuti-Hirayama formula,[23] $\log\{-\ln[I(t)/I_0(t)]\}$ shows a linear dependence on $\log(t)$ with slope of $3/s$ (Supporting Information, Formula S5). I(t) represents decay curve of the donor and $I_0(t)$ represents decay curve of donor in the absence of acceptor. s is a coefficient with value of 6, 8, and 10 respectively for dipole−dipole, dipole- quadrupole, and quadrupole−quadrupole interaction. As shown in Figure 4c,d, s is calculated to be 5.7 and 5.8 for Ce1−Ce2 and Ce1−Eu2, respectively.

Critical energy transfer distance R_0 is the distance between an isolated donor−acceptor pair, and that energy transfer rate is the same with the spontaneous radiation of donor. Energy transfer rate between Ce1 and Ce2 is marked as $W_{Ce1-Ce2}$. Energy transfer rate between Ce1 and Eu2 is marked as $W_{Ce1-Eu2}$. It can be proved that the ratio of energy transfer rate $W_{Ce1-Eu2}/W_{Ce1-Ce2}$ for an isolated Ce1−Ce2 pair and a Ce1−Eu2 pair with the same distance is equal to $(R_0^{Eu2}/R_0^{Ce2})^6$ (Supporting Information, Formula S2). R_0^{Ce2} is the critical distance for Ce1−Ce2, and R_0^{Eu2} is the critical distance for Ce1−Eu2. R_0^{Ce2} and R_0^{Eu2} is calculated to be 10.972 and 12.197 Å, respectively, based on the relation $R_0^6 = \alpha \times \tau_0$. α is a rate constant for energy transfer and is calculated through Inokuti−Hirayama formula (Supporting Information, Formula S7), as shown in Figure 5a,b. τ_0 is the lifetime of donor without

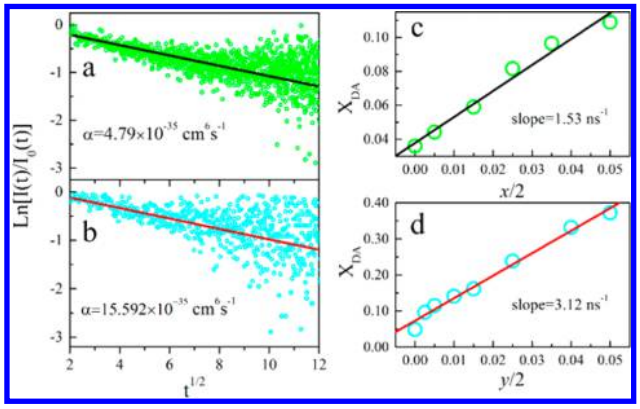

Figure 5. Plot of $\ln[I(t)/I_0(t)]$ vs $t^{1/2}$ for sample $SrAlSi_4N_7$:0.05Ce^{3+} (a) and $SrAlSi_4N_7$:0.05Ce^{3+},0.01Eu^{2+} (b) by monitoring 480 nm. Relationship between X_{DA} and acceptor concentration of $SrAlSi_4N_7$:$x$$Ce^{3+}$ (c) and $SrAlSi_4N_7$:0.05Ce^{3+},$y$$Eu^{2+}$ (d).

acceptors around. τ_0 for Ce1−Ce2 transfer is 36.4 ns, which is obtained by integrating the decay curve of $SrAlSi_4N_7$:0.001Ce^{3+}. τ_0 for Ce1−Eu2 transfer is 20.4 ns and is obtained from the decay of $SrAlSi_4N_7$:0.05Ce^{3+} by supposing that codoped Eu^{2+} ion will not change the energy transfer rate between Ce1−Ce2. Thus, $W_{Ce1-Eu2}/W_{Ce1-Ce2}$ is calculated to be 1.9.

At early regime of decay, the assumption that acceptors distribute continuously around the donor is invalid. Thus, the Inokuti−Hirayama model is no longer applicable. According to M. M. Broer's report,[24] the early regime instantaneous decay rate X_{DA} is (Supporting Information, Formula S9):

$$X_{DA} = m\sum_i W_{0i} + \frac{1}{\tau_0} \quad (4)$$

where m is the probability that site i is substituted by an acceptor, and W_{0i} is the energy transfer rate between a donor at site 0 and an acceptor at site i. For $SrAlSi_4N_7$:$x$$Ce^{3+}$, X_{DA} shows a linear dependence on $x/2$ with slope of $\sum_i W_{0i}^{Ce2}$. As shown Figure 5a, $\sum_i W_{0i}^{Ce2}$ equals 1.53 ns^{-1} based on the linear fitting. For decay curve with two acceptors X_{DA} can be derived to be (Supporting Information, Formula S10):

$$X_{DA} = \frac{1}{\tau_0} + m\sum_i W_{0i} + n\sum_i W'_{0i} \quad (5)$$

This formula is convenient to study the influence of each acceptor. In $SrAlSi_4N_7$:0.05Ce^{3+},$y$$Eu^{2+}$ samples, m is fixed, and X_{DA} is proportional to y. As shown in Figure 5b, $\sum_i W_{0i}^{Eu2}$ is 3.12 ns^{-1}. The ratio of $\sum_i W_{0i}^{Eu2}/\sum_i W_{0i}^{Eu2}$ is proved equal to $W_{Ce1-Eu2}/W_{Ce1-Ce2}$ (Supporting Information, Formula S12). Therefore, ratio of energy transfer rate $W_{Ce1-Eu2}/W_{Ce1-Ce2}$ is calculated to be 2.0. This result is accordance with the previous result ($W_{Ce1-Eu2}/W_{Ce1-Ce2}$ = 1.9) based on Inokuti−Hirayama formula. This result supports the assumption that low-concentration Eu^{2+} ion will not change the energy transfer rate between Ce1 and Ce2.

$W_{Ce1-Eu2}/W_{Ce1-Ce2}$ is inversely proportional to quadratic acceptor concentration c (Supporting Information, Formula S3). Thus, concentration of Eu2 (c^{Eu2}) is ∼2.5 times the of concentration of Ce2 (c^{Ce2}) to realize the same energy transfer rate between Ce1−Eu2 and Ce1−Ce2. This indicates that $W_{Ce1-Eu2}$ equals $W_{Ce1-Ce2}$ when y = 0.035 in $SrAlSi_4N_7$:0.05Ce^{3+},$y$$Eu^{2+}$ samples. When y > 0.035, $W_{Ce1-Eu2}$ is larger than $W_{Ce1-Ce2}$. As a result, energy transferred from Ce1 to Ce2 decreased. As shown in Table 1, the calculated results

Table 1. Calculated Total Energy Transfer Rate from Ce1 to Ce2, Eu2

$SrAlSi_4N_7$:$x$$Ce^{3+}$		$SrAlSi_4N_7$:0.05Ce^{3+},$y$$Eu^{2+}$			
x	$W_{Ce1-Ce2}$ (ns^{-1})	y	calculated[a] $W_{Ce1-Eu2}$ (ns^{-1})	calculated[b] $W_{Ce1-Ce2,Eu2}$ (ns^{-1})	measured $W_{Ce1-Ce2,Eu2}$ (ns^{-1})
0.05	0.44	0.005	0.01	0.45	0.49
		0.03	0.32	0.76	0.75
		0.04	0.57	1.01	0.80
		0.10	1.26	1.7	0.89

[a]Calculated according to formula S3 (Supporting Information). [b]Suppose energy transfer rate from Ce1 to Ce2 is a constant.

coincide with the experiments when $y \leq 0.03$ and diverge greatly when $y \geq 0.04$. This is in agreement with the calculated key point y = 0.035. This result indicates that high-concentration doped Eu^{2+} ion decreases the energy transfer rate between Ce1 and Ce2. This will decrease yellow component in the spectrum and, as a result, the yellow phosphor changes into a red one.

CONCLUSIONS

$SrAlSi_4N_7$:0.05Ce^{3+},$y$$Eu^{2+}$ is a highly color-tunable phosphor with emission shifting from 550 to 610 nm. There are three sub-bands, which can be ascribed to Ce1, Ce2, and Eu2, respectively, in the emission spectrum. Deconvolution of emission spectrum shows that Ce1 is a green luminescence center with a 530 nm emission, Ce2 is a yellow center with a

DOI: 10.1021/acs.inorgchem.6b01490
Inorg. Chem. 2016, 55, 9736−9741

580 nm emission, and Eu2 is a red center with a 630 nm emission. Thus, $SrAlSi_4N_7:Ce^{3+},Eu^{2+}$ is a desired phosphor for high CRI with green, yellow, and red components. However, energy transfer process is observed between Ce1−Ce2 and Ce1−Eu2. Such an energy transfer process is not desirable, since it reduces Ce1 intensity (green light). This further results in narrower FWHM and lower CRI of wLED. The competitive relation between Ce1−Ce2 and Ce1−Eu2 energy transfer processes is discussed in detail. Results show that Eu^{2+} ion controls the emission spectrum by Ce1−Eu2 energy transfer process. When Eu^{2+} concentration is low, Ce1−Eu2 transfer rate is low. The emission spectrum shows a little decrease of green component and evident increase of red component. This results in broader FWHM and higher CRI. With increasing Eu^{2+} concentration, Ce1−Eu2 transfer rate increases. This results in fast decrease of green component and narrower FWHM. Especially when $y > 0.035$, the green component is even undetectable, and the yellow phosphor changes into a red one. Although energy transfer between Ce1−Eu2 may be not anticipated, we can reduce the effect by controlling the concentration of Eu^{2+} ion. The best Eu^{2+} concentration is 0.01, and a wLED with CRI of 88 can be achieved. Phosphors with low-concentration doped Eu^{2+} are favorable to application in wLEDs requiring high CRI, while heavier-doped samples are in favor of wLEDs in need of low CCT.

■ ASSOCIATED CONTENT

Supporting Information

The Supporting Information is available free of charge on the ACS Publications website at DOI: 10.1021/acs.inorgchem.6b01490.

Derivations of formulas used herein (PDF)

■ AUTHOR INFORMATION

Corresponding Author

*E-mail: zhangjh@ciomp.ac.cn.

Notes

The authors declare no competing financial interest.

■ ACKNOWLEDGMENTS

This work was partially supported by the National Key R&D Program of China (Grant Nos. 2016YFB0701003 and 2016YFB0400605), National Natural Science Foundation of China (Grant Nos. 61275055, 11274007, 51402284, and 11604330), and the Natural Science Foundation of Jilin province (Grant Nos. 20140101169JC, 20150520022JH, and 20160520171JH).

■ REFERENCES

(1) Dai, P.; Li, C.; Zhang, X.; Xu, J.; Chen, X.; Wang, X.; Jia, Y.; Wang, X.; Liu, Y. A Single Eu^{2+}-Activated High-Color-Rendering Oxychloride White-Light Phosphor for White-Light-Emitting Diodes. *Light: Sci. Appl.* **2016**, *5*, e16024.

(2) Zhu, H.; Lin, C.; Luo, W.; Shu, S.; Liu, Z.; Kong, J.; Ma, E.; Cao, Y.; Liu, R.; Chen, X.; et al. Highly Efficient Non-Rare-Earth Red Emitting Phosphor for Warm White Light-Emitting Diodes. *Nat. Commun.* **2014**, *5*, 4312.

(3) Li, X.; Budai, J. D.; Liu, F.; Howe, J. Y.; Zhang, J.; Wang, X. J.; Gu, Z.; Sun, C.; Meltzer, R. S.; Pan, Z. New Yellow $Ba_{0.93}Eu_{0.07}Al_2O_4$ Phosphor for Warm-White Light-Emitting Diodes Through Single-Emitting-Center Conversion. *Light: Sci. Appl.* **2013**, *2*, e50.

(4) Lu, W.; Jiao, M.; Shao, B.; Zhao, L.; You, H. Enhancing Photoluminescence Performance of $SrSi_2O_2N_2:Eu^{2+}$ Phosphors by Re (Re = La, Gd, Y, Dy, Lu, Sc) Substitution and Its Thermal Quenching Behavior Investigation. *Inorg. Chem.* **2015**, *54*, 9060−9065.

(5) Song, K.; Zhang, J.; Liu, Y.; Zhang, C.; Jiang, J.; Jiang, H.; Qin, H. Red-Emitting Phosphor $Ba_9Lu_2Si_6O_{24}:Ce^{3+},Mn^{2+}$ with Enhanced Energy Transfer via Self-Charge Compensation. *J. Phys. Chem. C* **2015**, *119*, 24558−24563.

(6) Liu, Y.; Zhang, J.; Zhang, C.; Jiang, J.; Jiang, H. High Efficiency Green Phosphor $Ba_9Lu_2Si_6O_{24}:Tb^{3+}$: Visible Quantum Cutting via Cross-Relaxation Energy Transfers. *J. Phys. Chem. C* **2016**, *120*, 2362−2370.

(7) Zhang, L.; Zhang, J.; Zhang, X.; Hao, Z.; Zhao, H.; Luo, Y. New Yellow-Emitting Nitride Phosphor $SrAlSi_4N_7:Ce^{3+}$ and Important Role of Excessive AlN in Material Synthesis. *ACS Appl. Mater. Interfaces* **2013**, *5*, 12839−12846.

(8) Lin, Y. S.; Liu, R. S.; Cheng, B. M. Investigation of the Luminescent Properties of Tb^{3+}-Substituted YAG:Ce, Gd Phosphors. *J. Electrochem. Soc.* **2005**, *152*, J41−J45.

(9) Ayvacikli, M.; Canimoglu, A.; Muresan, L. E.; Barbu Tudoran, L.; Garcia Guinea, J.; Karabulut, Y.; Jorge, A.; Karali, T.; Can, N. Structural and Luminescence Effects of Ga Co-Doping on Ce-Doped Yttrium Aluminate Based Phosphors. *J. Alloys Compd.* **2016**, *666*, 447−453.

(10) Pan, Y.; Wu, M.; Su, Q. Tailored Photoluminescence of YAG:Ce Phosphor Through Various Methods. *J. Phys. Chem. Solids* **2004**, *65*, 845−850.

(11) Yang, H. K.; Jeong, J. H. Synthesis, Crystal Growth, and Photoluminescence Properties of $YAG:Eu^{3+}$ Phosphors by High-Energy Ball Milling and Solid-State Reaction. *J. Phys. Chem. C* **2010**, *114*, 226−230.

(12) Wang, L.; Zhang, X.; Hao, Z.; Luo, Y.; Zhang, L.; Zhong, R.; Zhang, J. Interionic Energy Transfer in $Y_3Al_5O_{12}$: Ce^{3+}, Pr^{3+}, Cr^{3+} Phosphor. *J. Electrochem. Soc.* **2012**, *159*, F68−F72.

(13) Jia, Y.; Huang, Y.; Zheng, Y.; Guo, N.; Qiao, H.; Zhao, Q.; Lv, W.; You, H. Color Point Tuning of $Y_3Al_5O_{12}$: Ce^{3+} Phosphor via Mn^{2+}−Si^{4+} Incorporation for White Light Generation. *J. Mater. Chem.* **2012**, *22*, 15146−15152.

(14) Shi, Y.; Wang, Y.; Wen, Y.; Zhao, Z.; Liu, B.; Yang, Z. Tunable Luminescence $Y_3Al_5O_{12}:0.06Ce^{3+}$, xMn^{2+} Phosphors with Different Charge Compensators for Warm White Light Emitting Diodes. *Opt. Express* **2012**, *20*, 21656−21664.

(15) Ye, S.; Xiao, F.; Pan, Y. X.; Ma, Y. Y.; Zhang, Q. Y. Phosphors in Phosphor-Converted White Light-Emitting Diodes: Recent Advances in Materials, Techniques and Properties. *Mater. Sci. Eng., R* **2010**, *71*, 1−34.

(16) Park, W.; Son, K.; Singh, S.; Sohn, K. Solid-State Combinatorial Screening of $ARSi_4N_7:Eu^{2+}$ (A = Sr, Ba, Ca; R = Y, La, Lu) Phosphors. *ACS Comb. Sci.* **2012**, *14*, 537−544.

(17) Ruan, J.; Xie, R.; Funahashi, S.; Tanaka, Y.; Takeda, T.; Suehiro, T.; Hirosaki, N.; Li, Y. A Novel Yellow-Emitting $SrAlSi_4N_7:Ce^{3+}$ Phosphor for Solid State Lighting: Synthesis, Electronic Structure and Photoluminescence Properties. *J. Solid State Chem.* **2013**, *208*, 50−57.

(18) Zhang, Z.; ten Kate, O. M.; Delsing, A.; Man, Z.; Xie, R.; Shen, Y.; Stevens, M.; Notten, P.; Dorenbos, P.; Zhao, J.; Hintzen, H. Preparation, Electronic Structure and Photoluminescence Properties of RE (RE = Ce, Yb)-Activated $SrAlSi_4N_7$ phosphors. *J. Mater. Chem. C* **2013**, *1*, 7856−7865.

(19) Zhang, Z.; ten Kate, O. M.; Delsing, A.; Dorenbos, P.; Zhao, J.; Hintzen, H. Photoluminescence Properties of Pr^{3+}, Sm^{3+} and Tb^{3+} doped $SrAlSi_4N_7$ and Energy Level Locations of Rare-Earth Ions in $SrAlSi_4N_7$. *J. Mater. Chem. C* **2014**, *2*, 7952−7959.

(20) Hecht, C.; Stadler, F.; Schmidt, P.; auf der Gunne, J. S.; Baumann, V.; Schnick, W. $SrAlSi_4N_7:Eu^{2+}$−A Nitridoalumosilicate Phosphor for Warm White Light (pc)LEDs with Edge-Sharing Tetrahedra. *Chem. Mater.* **2009**, *21*, 1595−1601.

(21) Ruan, J.; Xie, R.; Hirosaki, N.; Takeda, T. Nitrogen Gas Pressure Synthesis and Photoluminescent Properties of Orange-Red $SrAlSi_4N_7:Eu^{2+}$ Phosphors for White Light-Emitting Diodes. *J. Am. Ceram. Soc.* **2011**, *94*, 536−542.

DOI: 10.1021/acs.inorgchem.6b01490
Inorg. Chem. 2016, 55, 9736−9741

(22) Chen, L.; Liu, R.; Zhuang, D.; Liu, Y.; Hu, Y.; Zhou, X.; Ma, X. A Study on Photoluminescence and Energy Transfer of $SrAlSi_4N_7:Eu^{2+}$, Ce^{3+} Phosphors for Application in White-light LED. *J. Alloys Compd.* **2015**, *627*, 218−221.
(23) Inokuti, M.; Hirayama, F. Influence of Energy Transfer by the Exchange Mechanism on Donor Luminescence. *J. Chem. Phys.* **1965**, *43*, 1978−1989.
(24) Broer, M. M.; Huber, D. L.; Yen, W. M.; Zwicker, W. K. Resonant Fluorescence Line Narrowing in $La_{1-x}P_5O_{14}:xNd^{3+}$. *Phys. Rev. Lett.* **1982**, *49*, 394−398.

DOI: 10.1021/acs.inorgchem.6b01490
Inorg. Chem. 2016, 55, 9736−9741